Supporting Information for:

Concentration dependent salt-polymer-dynamic bond interactions dictate non-monotonic conductivity and viscoelasticity in vitrimer electrolytes

Samyak N. Chordia[1,2], Paul V. Braun[1,2], Shailesh N. Joshi[2,3], Timothy S. Arthur[4], Yu-Hsuan Tsao[1,2], Christopher M. Evans[1,2]*

[1]Department of Materials Science and Engineering and [2]Materials Research Laboratory, University of Illinois Urbana Champaign, Urbana, Illinois 61801, United States

[3]Electronics Research Department and [4]Materials Research Department, Toyota Research Institute of North America, Ann Arbor, Michigan 48105, USA

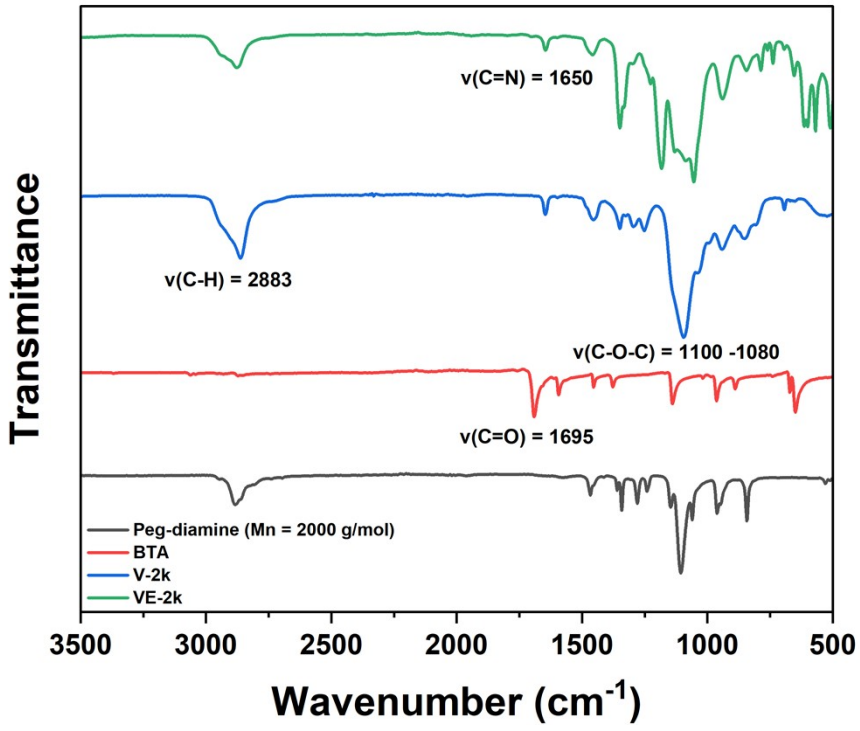

Figure S1. FTIR spectra of imine vitrimers shows presence of 1650 cm^{-1} peak, corresponding to imine bond stretch and disappearance of the aldehyde peak at 1695 cm^{-1} in neutral (V-2k) and salt-doped (VE-2k) networks indicating high conversion.

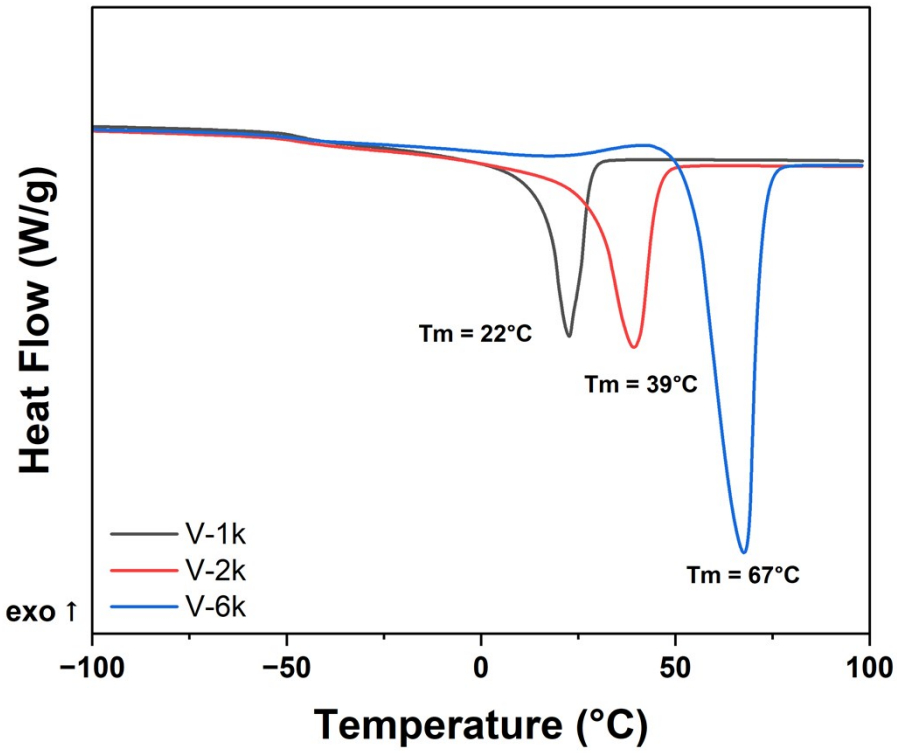

Figure S2. DSC curves for imine networks show a melting peak T_m, which increases with decreasing crosslinking density (longer EO chains). T_g values are observed at -50 °C for all the samples.

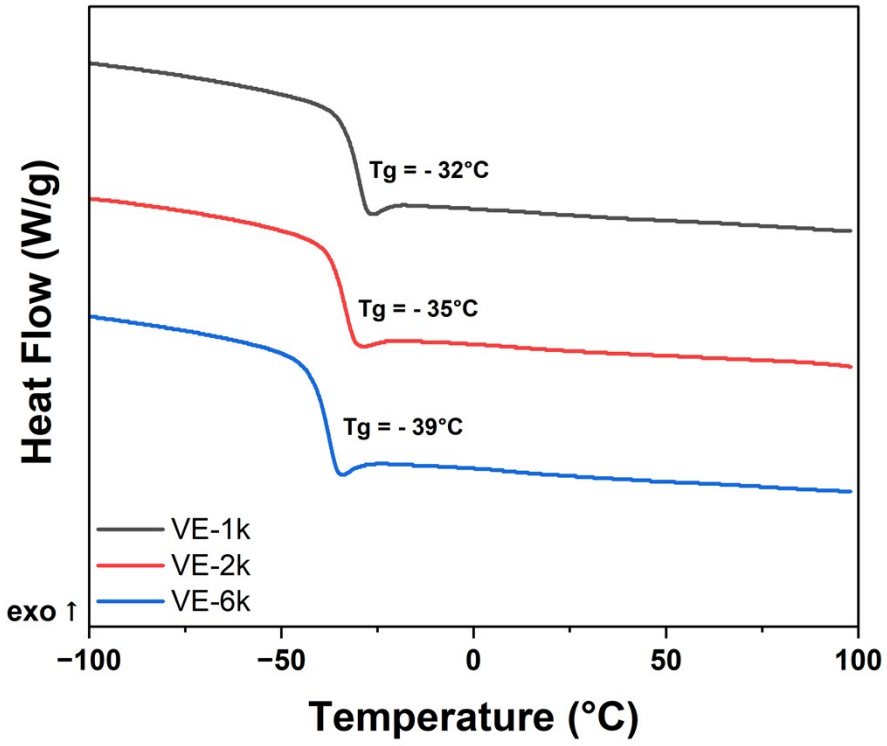

Figure S3. On salt addition, no T_m is observed and T_g increases relative to neutral vitrimers. T_g values increase with increasing crosslinking density.

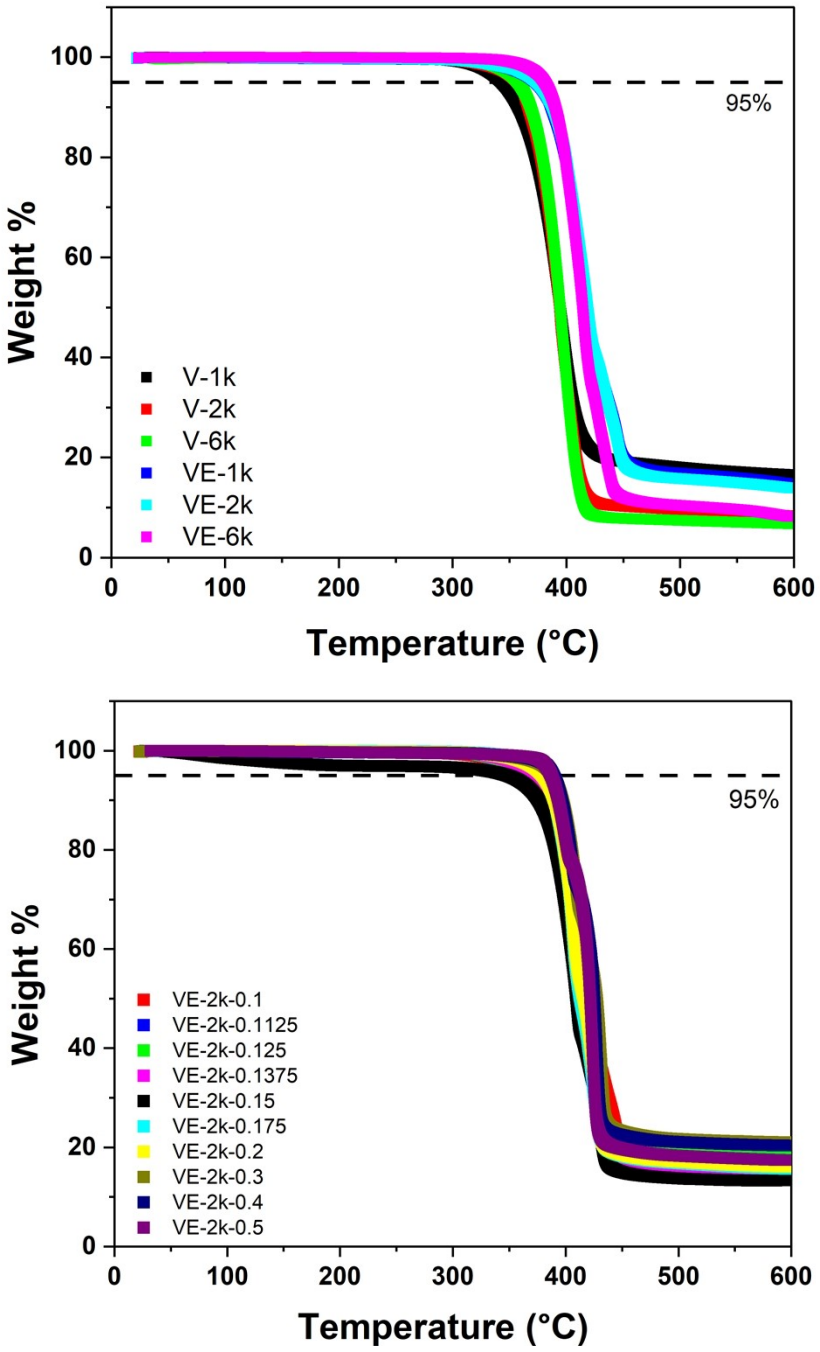

Figure S4. Thermal stability of vitrimer networks and electrolytes determined using thermo-gravimetric analysis. VEs show a higher onset of degradation (T_d) relative to V networks (**Table 1 and Table 2**)

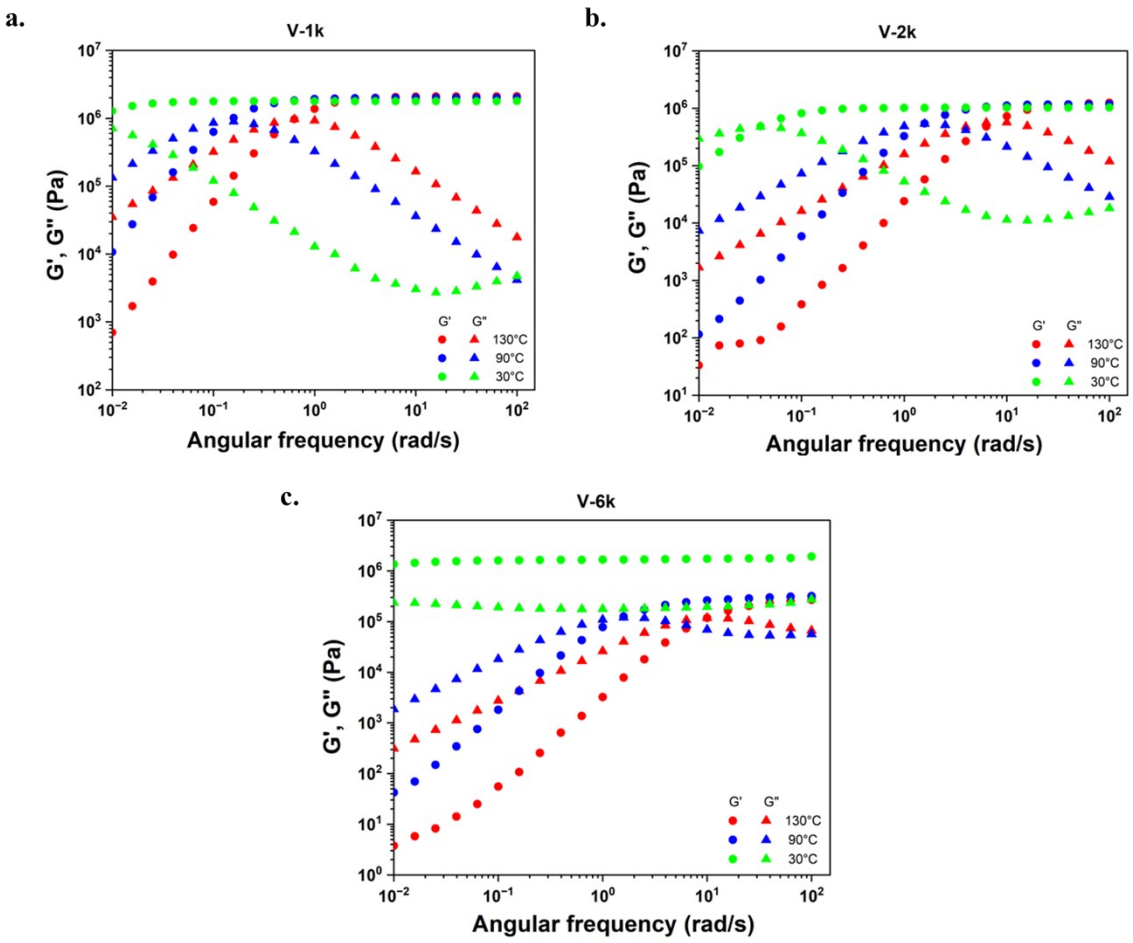

Figure S5. Frequency sweeps showing the storage modulus (G', solid circle symbols) and loss modulus (G'', solid triangle symbols) as a function of angular frequency from 130 °C to 30 °C for neutral vitrimers with varying crosslinking density (V-x). The plateau modulus increases with temperature as in permanent networks, except for V-6k sample which crystallizes below 50 °C.

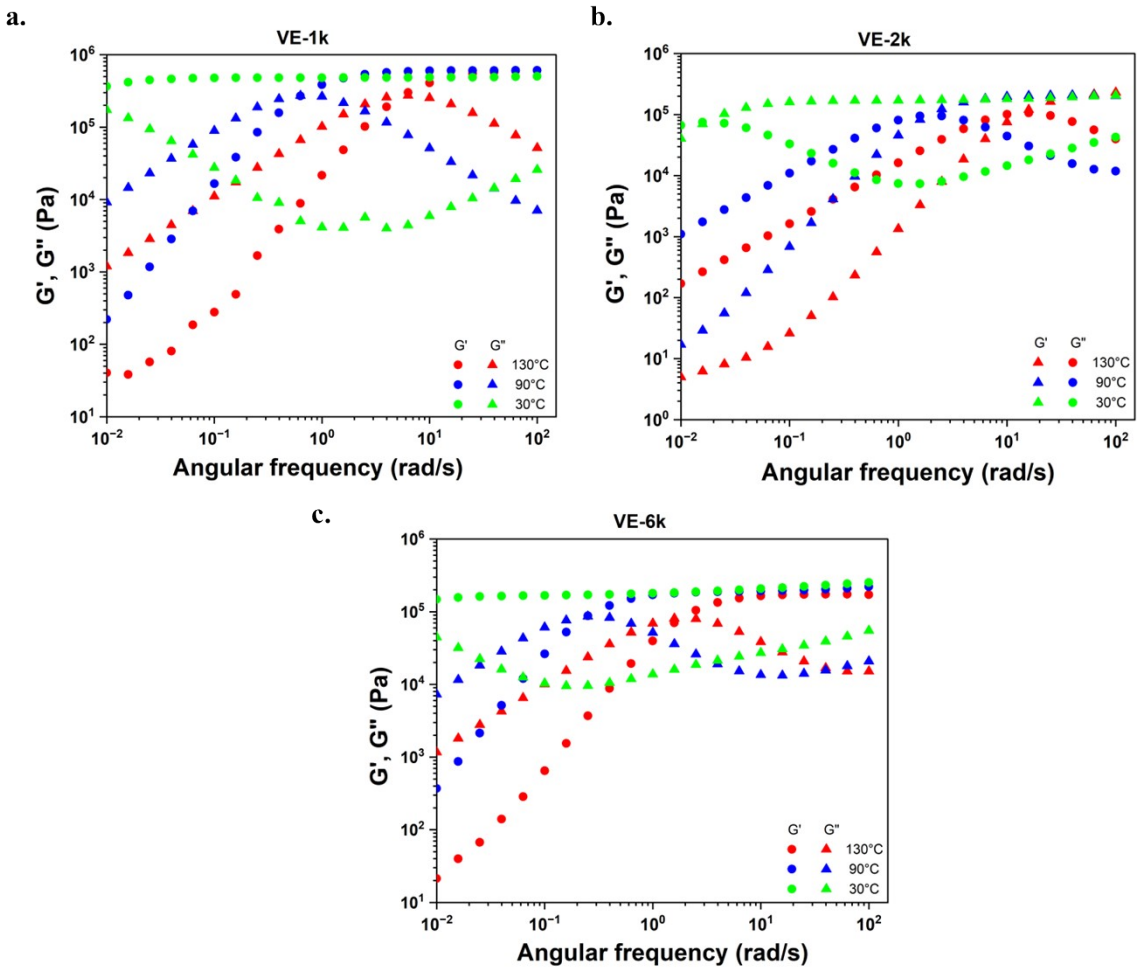

Figure S6 Frequency sweeps showing the storage modulus (G', solid circle symbols) and loss modulus (G'', solid triangle symbols) as a function of angular frequency from 130 °C to 30 °C for vitrimer electrolytes with varying crosslinking density (VE-x).

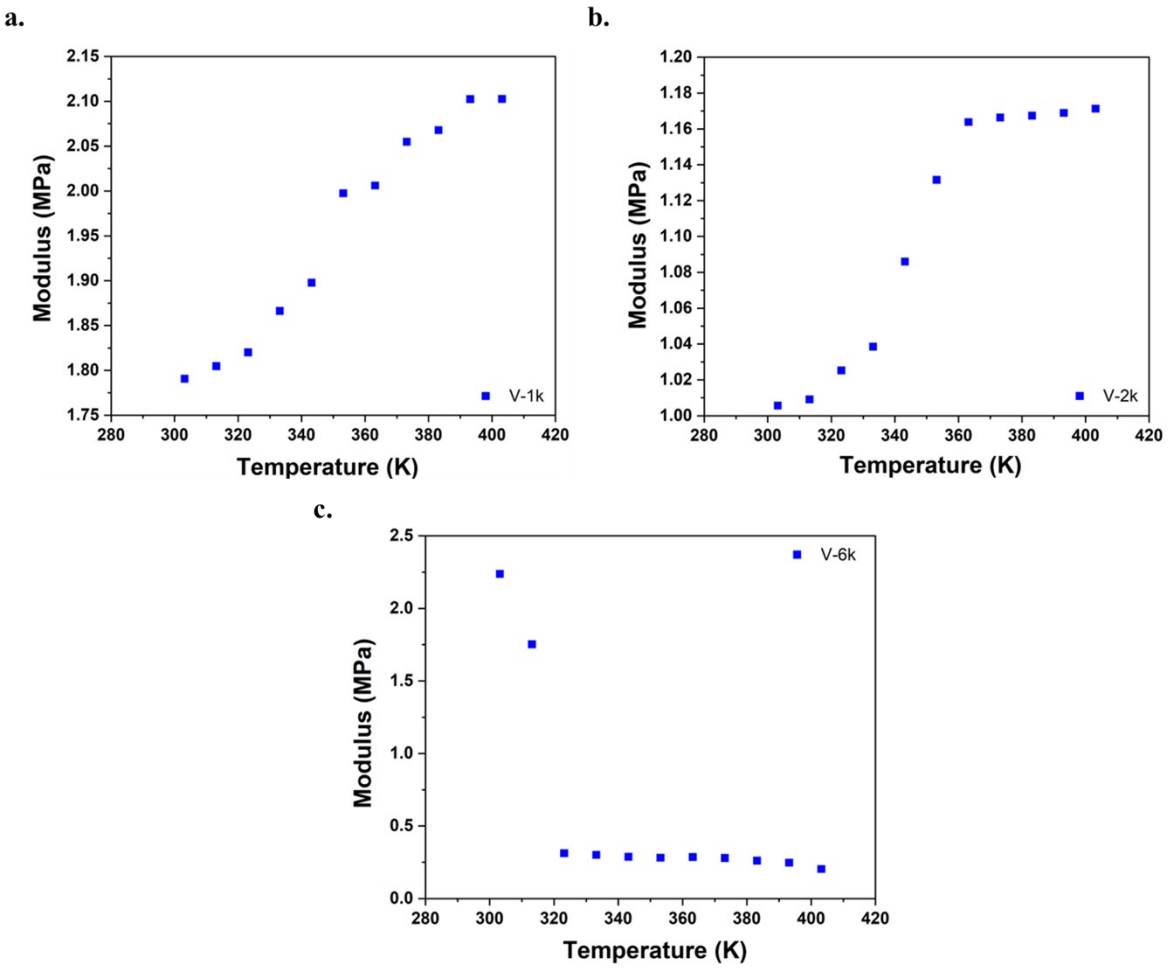

Figure S7. The shear modulus of the vitrimer networks increases linearly with increasing temperatures, indicating a conserved network topology. The plateau cannot be fully resolved in V-2k leading to non-linear deviations. V-6k crystallizes at lower temperatures leading to an increased modulus.

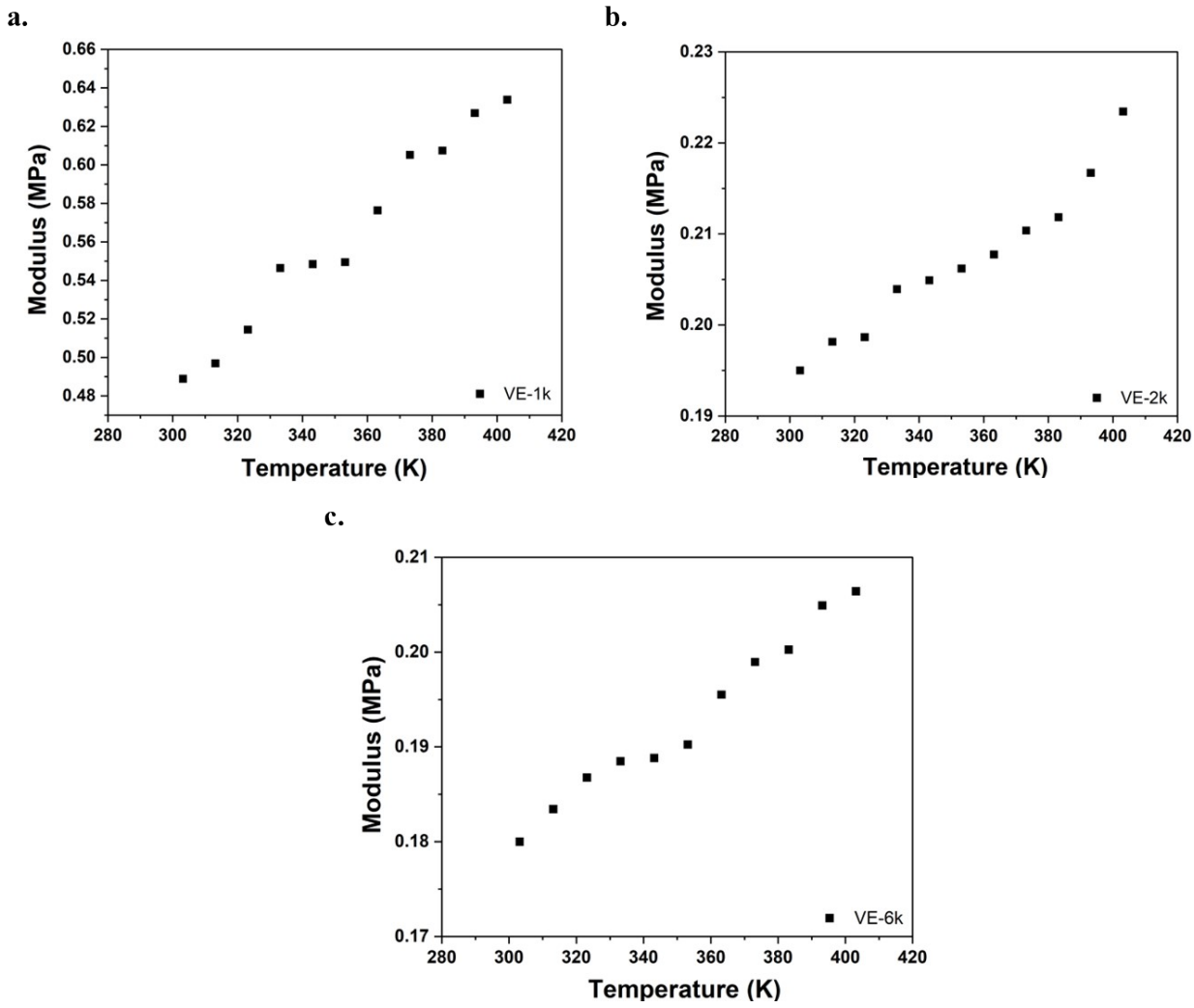

Figure S8. The shear modulus of the vitrimer electrolytes increases with increasing temperature, indicating a conserved network topology. Modulus also increases with crosslinking density.

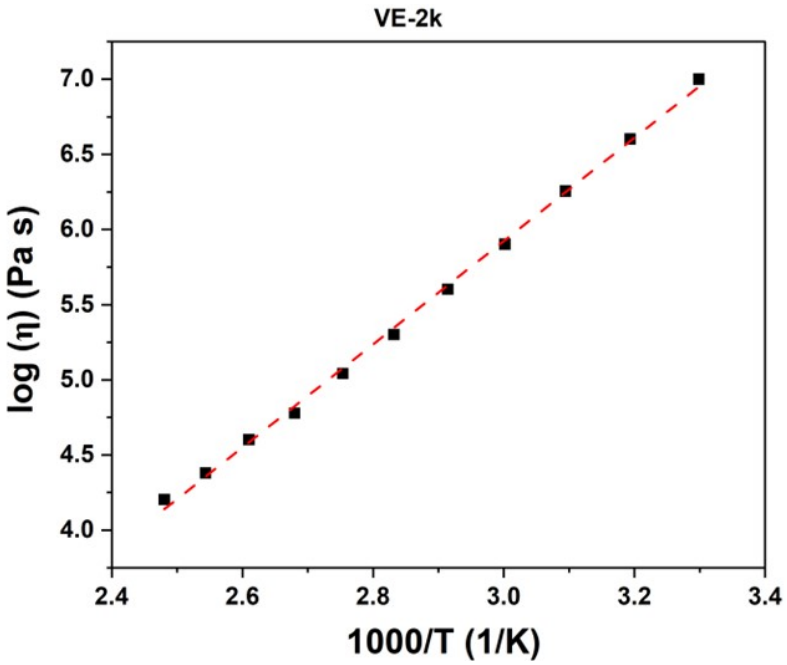

Figure S9. Viscosity values obtained from frequency sweep data show drop in magnitude with increasing temperature due to enhanced bond exchange. Calculated vitrimer temperature occurs at – 64 °C for VE-2k.

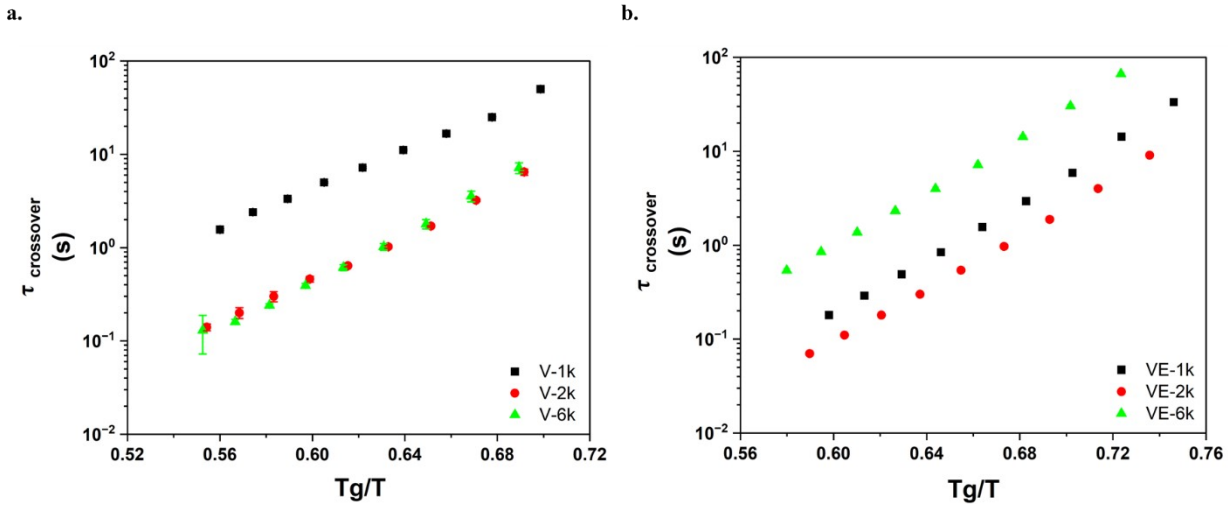

Figure S10. The crossover times do not collapse onto a single curve when plotted against normalized temperature T_g/T for networks **a.** without and **b.** with salt.

a.

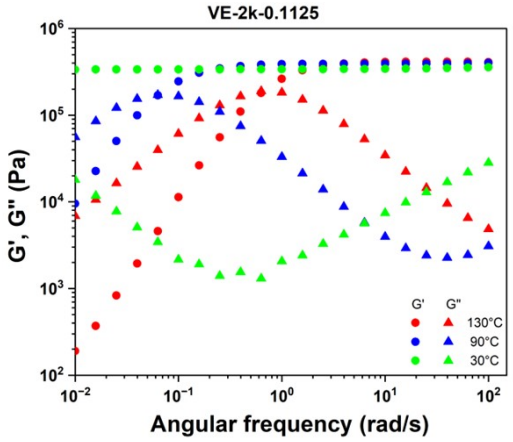
VE-2k-0.1125
G', G" (Pa)
Angular frequency (rad/s)
G'
G"
130°C
90°C
30°C

b.

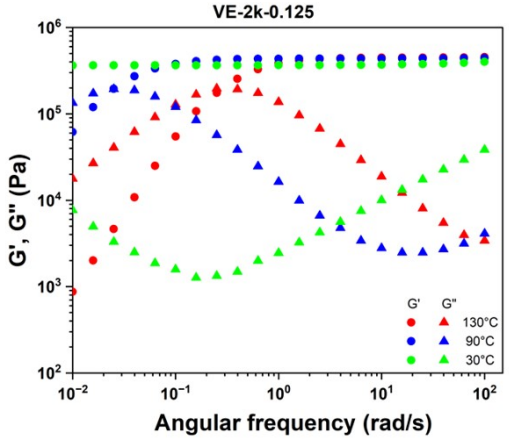
VE-2k-0.125
G', G" (Pa)
Angular frequency (rad/s)
G'
G"
130°C
90°C
30°C

c.

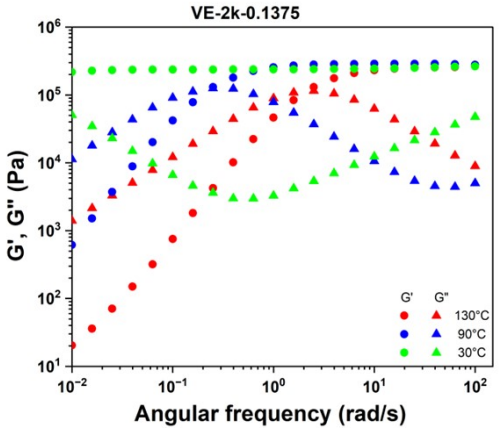
VE-2k-0.1375
G', G" (Pa)
Angular frequency (rad/s)
G'
G"
130°C
90°C
30°C

d.

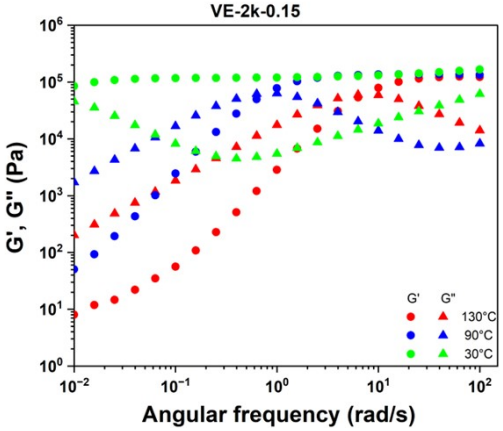
VE-2k-0.15
G', G" (Pa)
Angular frequency (rad/s)
G'
G"
130°C
90°C
30°C

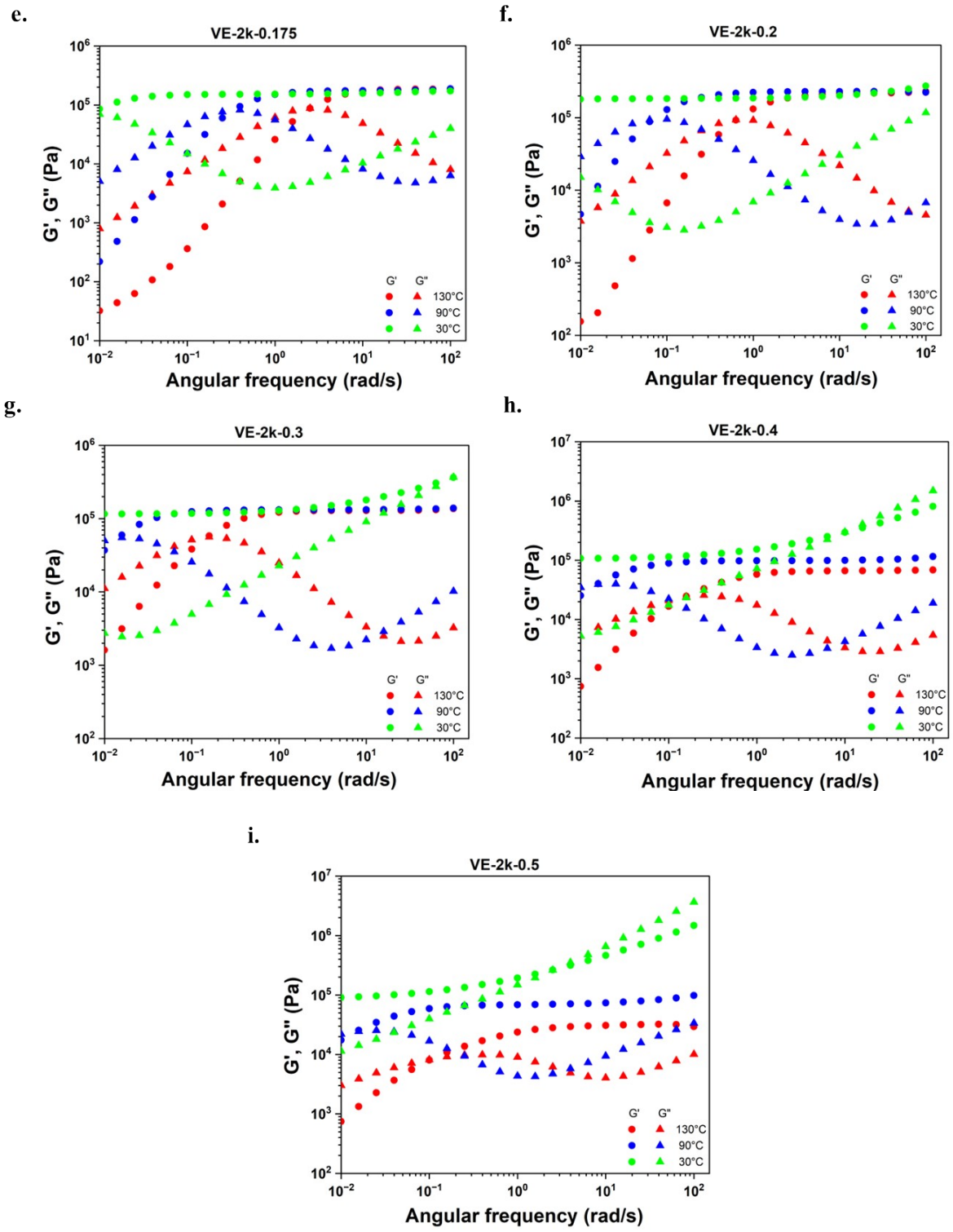

Figure S11. Frequency sweeps from 130°C to 30°C for VE-2k and r = 0.1 – 0.5.

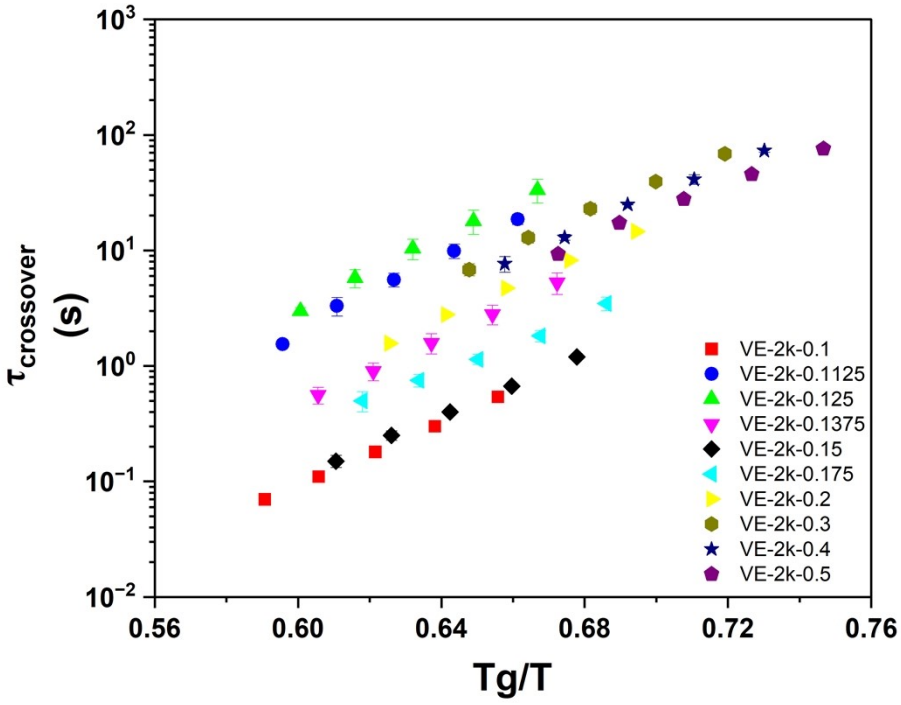

Figure S12. Crossover times do not overlap when plotted against normalized temperature for $r <$ 0.2 but begin to converge at higher salt concentrations.

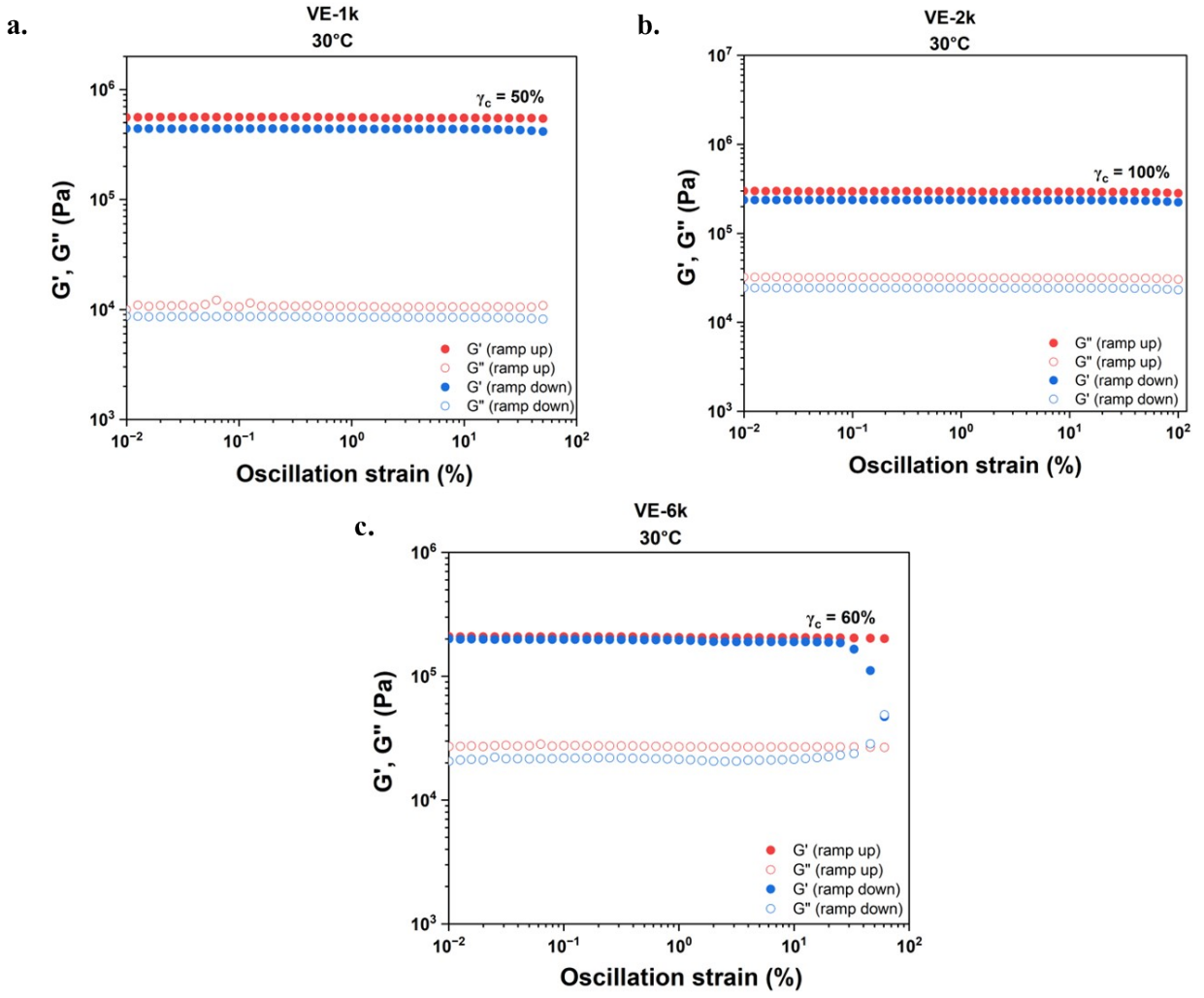

Figure S13a. Storage and loss modulus curves of VE-1k as a function of strain at 30 °C show good overlap during strain ramp up and ramp down cycles, indicating that the vitrimer electrolytes are not irreversibly disrupted by the LAOS measurements. **b.** VE-2k display highest critical strain (γ_c) of 100% with strain invariant modulus. **c.**VE-6k also shows good strain recovery with 60% critical strain.

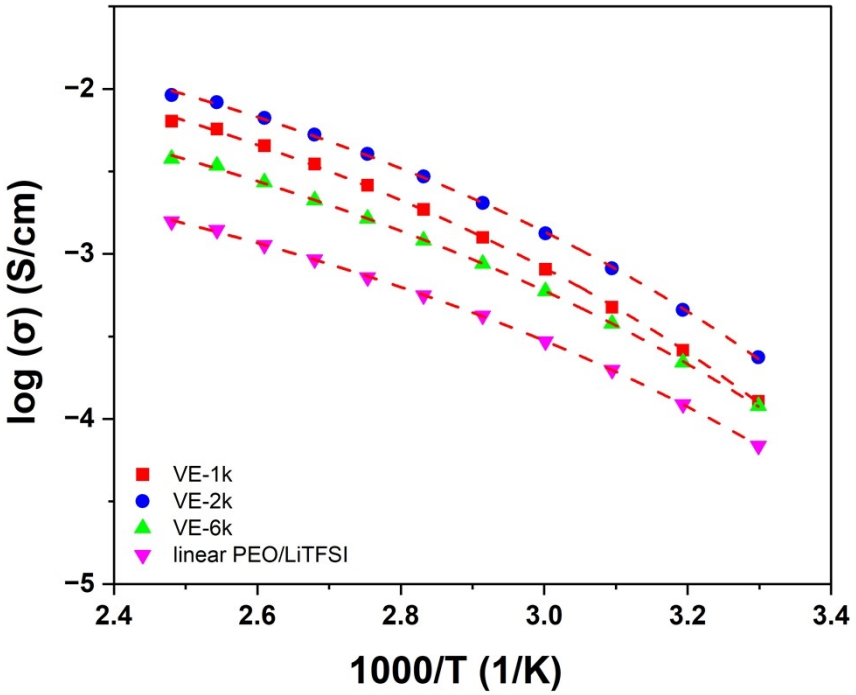

$$\text{VTF equation} - \ \sigma = \sigma_{\infty}\ \exp(-\frac{\text{DT0}}{\text{T} - \text{T0}})$$

Figure S14. Ionic conductivity of imine vitrimer electrolytes fitted by the Vogel-Tammann-Fulcher (VTF) equation as a function of different linker lengths (VE-x), indicating some degree of coupling between ion transport and segmental dynamics. σ_{∞} represents the limiting value of the conductivity at high temperature, D is the non-Arrhenius temperature dependence and T0 is the temperature at which the conductivity would converge to zero.

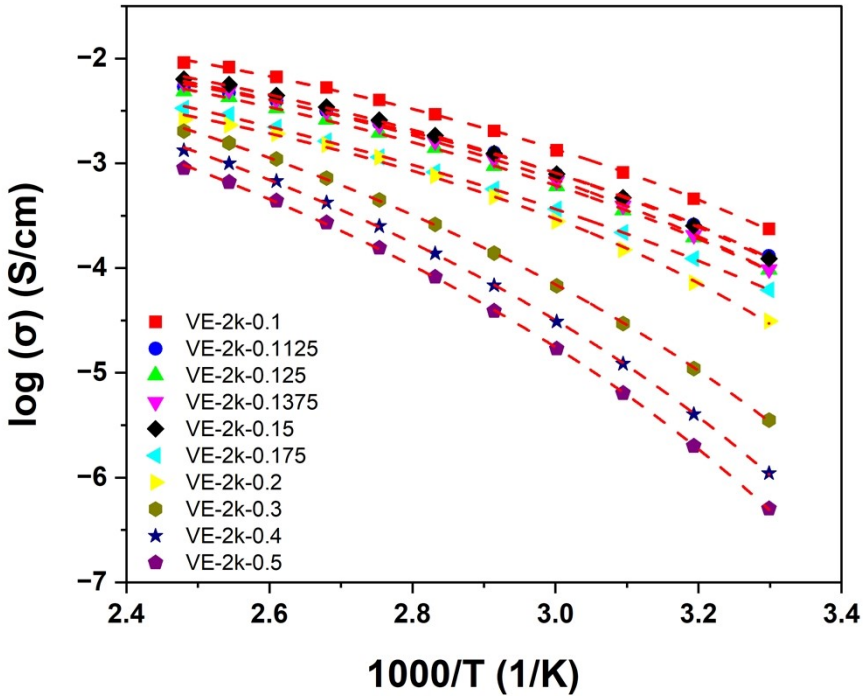

Figure S15. Ionic conductivity of imine vitrimer electrolytes fitted by the Vogel-Tammann-Fulcher (VTF) equation as a function of different salt concentrations (VE-2k-r).

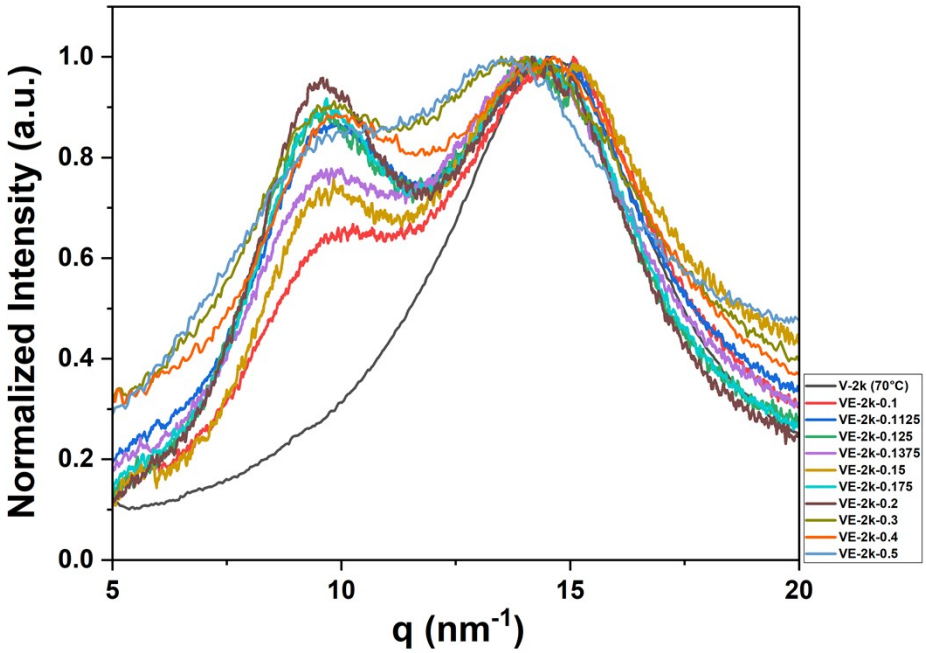

Figure S16. WAXS with an amorphous halo at q = 14.5 nm^{-1} and ionic aggregate peak at q = 9.5 nm^{-1}.

Figure S17. VE-2k-0.5 vitrimer electrolytes remains transparent despite high salt loading with no signs of salt-induced crystallization.

Table S1. VFT fit parameters for imine vitrimer electrolytes with varying crosslinking density (VE-x). No clear trends for D and T_0 are observed. σ_∞ shows similar non-monotonic trends as that of σ.

Samples	D	T_0 (K)	σ_∞ (S/cm)
VE-1k	1.52	209	0.27
VE-2k	1.35	212	0.3
VE-6k	1.56	201	0.14
PEO/LiTFSI	1.30	205	0.035

Table S2. VFT fit parameters for imine vitrimer electrolytes with varying salt concentrations (VE-2k-r). No clear trends for D, T_0 and σ_∞ are observed.

Samples	D	T_0 (K)	σ_∞ (S/cm)
VE-2k-0.1	1.35	212	0.3
VE-2k-0.1125	1.12	221	0.13
VE-2k-0.125	1.56	208	0.23
VE-2k-0.1375	1.41	214	0.24
VE-2k-0.15	1.48	210	0.28
VE-2k-0.175	2.67	180	0.5
VE-2k-0.2	1.15	228	0.09
VE-2k-0.3	2.6	206	1.11
VE-2k-0.4	2.7	209	1.18
VE-2k-0.5	2.86	209	1.18